Proceedings of the 36th Chinese Control Conference
July 26-28, 2017, Dalian, China

Sliding Mode High Speed Control of PMSM for Electric Vehicle Based on Flux-weakening Control Strategy

Dong Guo[1,2], Venkata Dinavahi[2], Qi Wu[1], Wei Wang[1]

1. School of Electrical Engineering, Liaoning University of Technology, Jinzhou 121000, China
E-mail: guocn99@163.com

2. Department of Electrical and Computer Engineering, University of Alberta, Edmonton T6G2V4, Canada
E-mail: mail: dinavahi@ualberta.ca

Abstract: To broaden the speed range of PMSM (Permanent Magnet Synchronous Motor) for the electric vehicles and to improve the stability in the high speed and small torque operating conditions of the electric vehicles, the control strategy based on flux-weakening control algorithm, using voltage feedback method, combined with SMVSC (Sliding Mode Variable Structure Control) algorithm, using the improved exponential reaching law and variable rate reaching law, is applied to the vector control system of PMSM for the electric vehicles. To solve the hysteretic nature caused by the introduction of integral link to the SMVSC algorithm, the method of the integral signal times the saturation function is adopted. Then the response speed and stability of the system are improved. Simulation results show that the good anti-jamming capability is achieved and the working conditions requirement of wide speed range is met.

Key Words: sliding mode variable structure control, flux-weakening control, speed control, permanent magnet synchronous motor, electric vehicles

1 Introduction

Motor drive control system is the key technology of the electric vehicles. Permanent magnet synchronous motor is widely used in electric vehicles because of its high power density, high efficiency and other advantages. Due to the simple and stable characteristics, PI vector control method is used in the PMSM control system [1, 2]. But PMSM control system is a nonlinear and strongly coupled multivariable system. PI vector control method cannot meet the requirements of high performance control when the PMSM control system is subjected to external disturbance. Hence many modern control methods, such as neural network, fuzzy control and SMVSC, have been applied to the PMSM speed control system in order to improve the stability of the electric vehicles at high speed [3, 4]. SMVSC is a kind of special nonlinear control algorithm, and it has the advantages of fast response, insensitive to disturbance and variable parameters. In [5-7], a sliding mode variable structure controller with dynamic sliding surface is designed, which makes the system have fast response and well stability. In [8], a SMVSC strategy with a novel exponential reaching law is applied to the PMSM vector control system. And dynamic and static performance of the system is improved. Meanwhile, in order to broaden the speed range of PMSM for the electric vehicles to meet the operating conditions of high-speed running, overtaking, and so on, many flux-weakening control methods have been proposed [9-13]. In [9], a compensation method based on the d-axis current of the PMSM is presented. In [10], a leading angle flux-weakening control method of PMSM is used in electric vehicles. In [11], a method of modifying the current set point is proposed. In [12], an approach to flux-weakening control of PMSM is presented, accounting for resistive voltage drop. The control strategy is based on a feed forward scheme, with the d-q current references computed from the PMSM model as a function of the speed and the current and voltage feeding limits.

In this paper, the speed controller is designed based on SMVSC algorithm with the improved exponential reaching law and variable rate reaching law. The control strategy based on flux-weakening control algorithm and SMVSC algorithm is applied to the vector control system of PMSM. Hence, speed range is broadened widely and the stability under the high-speed and small torque operating conditions of the electric vehicles is improved.

2 PMSM Model

Surface mounted PMSM is selected in this research. The following assumptions are made to derive the dynamic model of the PMSM for electric vehicle:

(1) Motor parameters and rotor PM flux are constant;

(2) The rotor magnetic field distributed in the space of air gap is sinusoidal;

(3) Induction electromotive force is sinusoidal;

(4) The magnetic circuit is linear. The core saturation and the core eddy current and hysteresis losses are neglected.

The dynamic model of the permanent magnet synchronous machine (PMSM) is derived using a two-phase motor in direct and quadrature (hereafter referred to as d-q) axes. This approach is desirable because of the conceptual simplicity obtained with only one set of two windings on the stator and leads to a control of the PMSM drive that is equivalent to the control of dc machines; a concept is known as vector control. Through Clark and Park transformation, the motor phase currents are equivalent to i_d and i_q . i_d can be seen as demagnetic current; i_q can be seen as the torque current that is relevant with the PMSM speed. So, the speed control can be realized through controlling i_q when $i_d = 0$ directly.

*This work is supported by National Natural Science Foundation (NNSF) of China under Grant 51275021, Natural Science Foundation of Liaoning Province 201602370, General research project of Liaoning Provincial Department of Education L2015229.

The voltage equation of PMSM under the d-q coordinate is shown as (1) [14].

$$\begin{cases} u_{\mathrm{d}} = R_{\mathrm{s}} i_{\mathrm{d}} + L_{\mathrm{d}} \dfrac{di_{\mathrm{d}}}{dt} - \omega L_{\mathrm{q}} i_{\mathrm{q}} \\ u_{\mathrm{q}} = R_{\mathrm{s}} i_{\mathrm{q}} + L_{\mathrm{q}} \dfrac{di_{\mathrm{q}}}{dt} + \omega L_{\mathrm{d}} i_{\mathrm{d}} + \omega \psi_{\mathrm{f}} \end{cases} \tag{1}$$

Where, u_{d} and u_{q} are the d-axis and q-axis voltage in the synchronous rotating reference frame, respectively; i_{d} and i_{q} are the d-axis and q-axis current, respectively; L_{d} and L_{q} are d-axis and q-axis inductance, respectively; R_{s} is the stator phase resistance; ψ_{f} is the flux linkage; ω is the electrical rotor speed.

The electromagnetic torque is given by

$$T_{\mathrm{e}} = 1.5 p \psi_{\mathrm{f}} i_{\mathrm{q}} \tag{2}$$

Where, T_{e} is the electromagnetic torque, N·m; p is the number of poles of PMSM.

The equation of motion can be written as

$$T_{\mathrm{e}} - T_{\mathrm{L}} = \frac{J}{p} \cdot \frac{d\omega}{dt} \tag{3}$$

Where, T_{L} is the load torque, N·m; J is the total moment of inertia, kg·m^2; ω is the electrical rotor speed, rad/s.

3 Principle of flux-weakening control

The flux-weakening control method of PMSM comes from the speed regulating control of a separately excited DC motor. In order to achieve higher speed in the condition of constant power, the excitation current of the DC motor should be reduced to keep the voltage balance when the terminal voltage of the separately excited DC motor reaches the limit voltage. Flux-weakening for speed expansion can be realized through reducing the excitation current of the DC motor. Because the excitation magneto motive force produced by permanent magnet of PMSM cannot be adjusted, the objective of flux-weakening for speed expansion can only be achieved through adjusting the stator current to increase the d-axis demagnetization current to maintain the voltage balance in the high speed condition.

Due to the limited capacity of the inverter, the current and the voltage limit can be expressed as [15]

$$i_{\mathrm{d}}^{\,2} + i_{\mathrm{q}}^{\,2} \le I_{\mathrm{smax}}^{\,2} \tag{4}$$

$$u_{\mathrm{d}}^{\,2} + u_{\mathrm{q}}^{\,2} \le U_{\mathrm{smax}}^{\,2} \tag{5}$$

Where, I_{smax} and U_{smax} represent maximum current and maximum voltage of the inverter.

When PMSM is in the high speed condition, the resistance drop can be neglected. Then the voltage equation of PMSM can be rewritten as

$$u_{\mathrm{s}}^{\,2} = (\omega L_{\mathrm{q}} i_{\mathrm{q}})^2 + (\omega L_{\mathrm{d}} i_{\mathrm{d}} + \omega \psi_{\mathrm{f}})^2 \tag{6}$$

Where,

$$u_{\mathrm{s}}^{\,2} \le U_{\mathrm{smax}}^{\,2} \tag{7}$$

Because of SMPMSM, $L_{\mathrm{d}} = L_{\mathrm{q}} = L_{\mathrm{s}}$, then it can be got from (6) and (7)

$$(i_{\mathrm{d}} + \frac{\psi_{\mathrm{f}}}{L_{\mathrm{s}}})^2 + (i_{\mathrm{q}})^2 \le (\frac{U_{\mathrm{smax}}}{\omega L_{\mathrm{s}}})^2 \tag{8}$$

From (4), (5) and (8), it can be known that the current limit condition is represented as a circle whose center is origin and radius is the maximum current, I_{smax}, and the voltage limit condition is a circle whose center is $(-\psi_{\mathrm{f}}/L_{\mathrm{s}}, 0)$ and radius is inversely proportional to the rotating speed in the current plane. Optimal current for the maximum output is shown in the Fig.1.

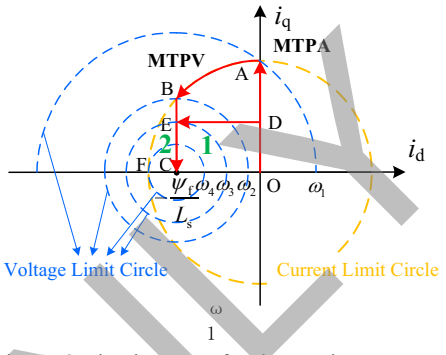

Fig. 1: Optimal current for the maximum output

Fig.1 shows the voltage limit and the current limit in the current plane with various speed, and the current trajectory for maximum torque. In the region that the speed is lower than ω_1, the maximum current is the only limiting condition that affects the operating region. Under the base speed, PMSM runs in the constant torque region. And the maximum electromagnetic torque can be obtained through using the MTPA (Maximum Torque Per Ampere) control, which is shown as the curve OA. As the speed increases, when the stator voltage exceeds the limit voltage that the inverter can withstand, the operation point of PMSM is on the constant torque curve between the MTPA curve OA and the MTPV (Maximum Torque Per Voltage) curve BC. The constant torque curves (curve DE as an example) parallel to the d-axis, and the region is called as the flux-weakening region 1 (FWR1). And the speed ω_1 is called as base speed of PMSM. If the center of the voltage-limit-circle lies in the circle of the current limit, as in Fig.1, from the speed over ω_2, the maximum torque point is not on the current-limit-circle, but on the MTPV line. The region between curve BC and BF is called as the flux-weakening region 2 (FWR2). Different control method should be adopted in the FWR1 and FWR2. In the flux-weakening process, the most thing is to determine how to correct the current reference.

4 Design of speed controller

4.1 Establish the state space equation

The state variable of PMSM control system can be represented as (9).

$$\begin{cases} x_1 = \omega^* - \omega \\ x_2 = \dfrac{dx_1}{dt} = -\dfrac{d\omega}{dt} \end{cases} \tag{9}$$

Where, ω^* is the speed reference; ω is the electrical rotor speed.

Then the expression is derived through (2) (3) (9).

$$\begin{cases} \dfrac{dx_1}{dt} = -\dfrac{d\omega}{dt} = \dfrac{p}{J}(1.5p\psi_f i_q - T_L) \\ \dfrac{dx_2}{dt} = -\dfrac{d^2\omega}{dt} = -1.5\dfrac{p^2}{J}\psi_f \dfrac{di_q}{dt} \end{cases} \tag{10}$$

Define $D = 1.5\dfrac{p^2}{J}\psi_f$ and $U = \dfrac{di_q}{dt}$, then the system state space equation is rewritten as

$$\begin{bmatrix} \dfrac{dx_1}{dt} \\ \dfrac{dx_2}{dt} \end{bmatrix} = \begin{bmatrix} 0 & 1 \\ 0 & 0 \end{bmatrix}\begin{bmatrix} x_1 \\ x_2 \end{bmatrix} + \begin{bmatrix} 0 \\ -D \end{bmatrix} U \tag{11}$$

4.2 Select SMVSC surface

One order linear SMVSC surface is selected.

$$s = cx_1 + x_2 \qquad (c > 0) \tag{12}$$

Then the derivative is obtained as

$$\frac{ds}{dt} = c\frac{dx_1}{dt} + \frac{dx_2}{dt} = cx_2 - DU \tag{13}$$

4.3 Select reaching law

Variable exponent reaching law can be written as

$$\frac{ds}{dt} = -\varepsilon |x_1| \operatorname{sgn}(s) - qs \tag{14}$$

Where, $\varepsilon |x_1|$ is exponential reaching law, $\varepsilon > 0$; qs is variable rate reaching law, $q > 0$.

4.4 Analyze the stability

According to Lyapunov stability theory, the condition of the existence and accessibility of SMVSC is

$$\dot{V}(x) = s\dot{s} < 0 \tag{15}$$

Where, $s \neq 0$; $V(x)$ is Lyapunov function, $V(x) = \dfrac{1}{2}s^2$.

Then the substitution of Equations (13) and (14) into Equation (15) results in

$$\dot{s}s = -\varepsilon |x_1||s| - qs^2 \le 0 \tag{16}$$

So Equation (16) is always set up whatever the value of s is.

4.5 Get the control rate

According to Equations (12) and (14), the output expression of controller can be written as

$$U = \frac{1}{D}[cx_2 + \varepsilon |x_1| \operatorname{sgn}(s) + qs] \tag{17}$$

Then q-axis current reference is written as

$$i_q = \frac{1}{D}\int [cx_2 + \varepsilon |x_1| \operatorname{sgn}(s) + qs]dt \tag{18}$$

4.6 Improve the control rate

Because sgn(s) is a discontinuous function, the chattering appears during the switching process. Then sgn(s) is substituted by $sat(s,\delta)$. The expression of $sat(s,\delta)$ is shown as below.

$$sat(s,\delta) = \begin{cases} 1, & s > \delta \\ s/\delta, & |s| < \delta \\ -1, & s < -\delta \end{cases} \tag{19}$$

Where, δ is a small positive constant.

So (18) can be written as

$$i_q = \frac{1}{D}\int (cx_2 + \varepsilon |x_1| sat(s,\delta) + qs)dt \tag{20}$$

In order to eliminate the effect of integral, the expression of i_q is improved as

$$i_q = \frac{1}{D}\int (cx_2 + \varepsilon |x_1| sat(s,\delta) + qs)dt \times sat(s,\delta) \tag{21}$$

5 Design of control strategy

According to the above, the control strategy based on flux-weakening control algorithm, using voltage feedback method, combined with SMVSC algorithm using the improved exponential reaching law and variable rate reaching law is applied to the vector control system of PMSM. The control strategy block diagram is shown as Fig.2.

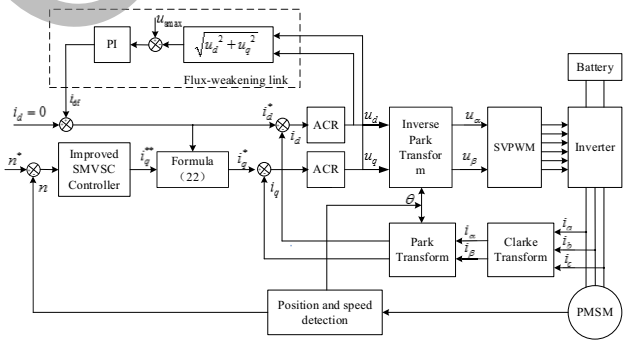

Fig. 2: Control strategy block diagram

In Fig.2, based on the $i_d = 0$ vector control system, the voltage feedback value, $\sqrt{u_d^2 + u_q^2}$, is represented by the d-axis given reference voltage and the q-axis given reference voltage which are the output of the ACR regulator, respectively. To check whether the operation point of PMSM is in the flux-weakening control region or not, the operation state of PMSM can be determined through the compare of the voltage feedback value $\sqrt{u_d^2 + u_q^2}$ with the given reference voltage u_{smax}, where $u_{smax} = k_u \times U_{dc}$ (k_u is the proportional coefficient). The given reference voltage value u_{smax} is related to the DC voltage of battery and PWM control method. If SVPWM (Space Vector Pulse Width Modulation) method is utilized, k_u is set to 0.577 in order to ensure that the output voltage does not exceed the hexagon

boundary of SVPWM control method. In the actual system, because of the current harmonic, the voltage loss of the inverter and the additional voltage drop caused by the current regulator and current integral, u_{smax} of the voltage loop will be less than $U_{dc}/\sqrt{3}$. So the selection range of k_u is [0.5, 0.577]. Because U_{dc}=192V here, u_{smax}=96V.

When in the flux-weakening control region, the d-axis demagnetization current i_d of the stator is obtained from the PI regulator according to the error between the voltage feedback value $\sqrt{u_d^2+u_q^2}$ and the given reference voltage u_{smax}. And the condition $i_d<0$ is realized. Hence the objective of flux-weakening for speed expansion is achieved. The q-axis given reference current is described as follow.

$$i_q^* = \mathrm{sgn}(i_q^{**})\sqrt{i_q^{**2}-i_d^{*2}} \tag{22}$$

Where,

$$\mathrm{sgn}(i_q^{**}) = \begin{cases} 1, & i_q^{**} \geq 0 \\ -1, & i_q^{**} < 0 \end{cases} \tag{23}$$

6 Simulation analysis

According to the control strategy block diagram in Fig.2, the system simulation model is set up under Simulink.

Based on consulting data and the manufacture, the parameters of PMSM for the electric vehicles in this research is shown in Table 1.

Table 1: The parameters of PMSM

Title	Parameters
Rated power P_N (kW)	7.5
Rated speed n_N (rpm)	3000
Rated torque T_N (N·m)	24
Stator phase resistance R_s (Ω)	0.025
Total moment of inertia J (kg·m²)	0.01
d-axis inductance L_d (mH)	0.985
q-axis inductance L_q (mH)	0.985
Flux linkage ψ_f (Wb)	0.062
Number of poles	4

6.1 Simulation analysis under speed changing condition

The performance of control strategy is investigated through the speed changing simulation in the above base speed and different load starting condition. Simulation parameters are set as follows.

(1) Light load starting condition

t=0, n^*=3000, T_L= 5; t=0.6, n^*=5000, T_L= 5

(2) Rated load starting condition

t=0, n^*=3000, T_L= 24; t=0.6, n^*=5000, T_L= 5

(3) Heavy load starting condition

t=0, n^*=1800, T_L= 40; t=0.6, n^*=5000, T_L= 5

In the heavy load starting condition, according to energy conversation principle, when T_L=40 N·m, the speed of PMSM cannot reach 3000rpm. Hence, according to (24), n^* is set as 1800.

$$n = 9550 * P_N / T_L \tag{24}$$

Speed response curves comparison between SMVSC and PI control strategy of the speed changing simulation in the high speed condition are shown in Fig.3.

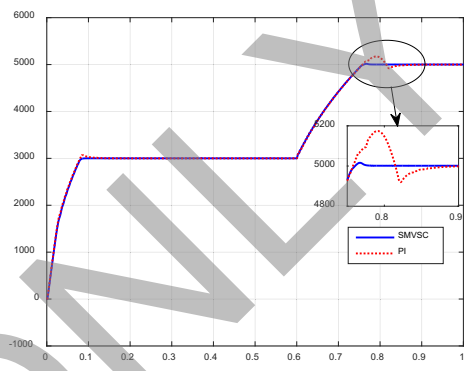

(a) Light load starting condition

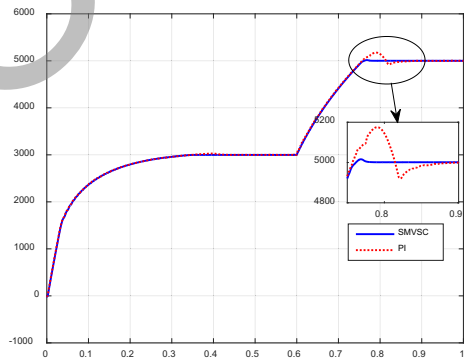

(b) Rated load starting condition

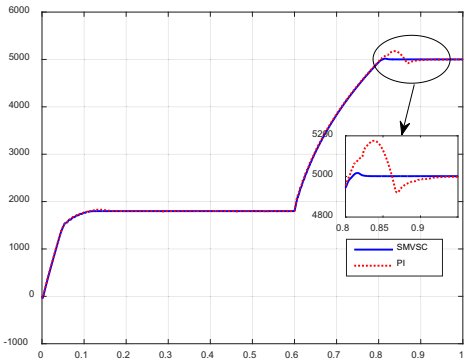

(c) Heavy load starting condition

Fig. 3: Speed response curves comparison in the speed changing condition

Performance parameters in different operating conditions and simulated using different control strategies are shown in Table 2. From Fig.3 and Table 2, it can be known that the SMVSC and flux-weakening control strategy shows better

performance than PI control strategy at transient. Less overshoot and less setting time are realized. Better control performance and better response speed of the PMSM system are achieved through applying the SMVSC and flux-weakening control strategy.

Table 2: Performance parameters in different operating conditions and different control strategies

	Light load	Rated load	Heavy load
Overshoot(PI)	2.18%	2.18%	2.18%
Overshoot(SMVSC)	0.2%	0.2%	0.2%
Settling time(PI)	0.224s	0.224s	0.272s
Settling time (SMVSC)	0.176s	0.176s	0.22s

6.2 Analysis of interference in high speed condition

The performance of control strategy is investigated through the sudden load interference simulation in the above base speed condition. Simulation parameters are set as follows.

t=0, n^* =3000, T_L= 5

t=0.4, n^* =5000, T_L= 5

t=0.8, n^* =5000, T_L= 14

Speed response curves comparison between SMVSC and PI control strategy of interference in high speed condition are shown in Fig.4.

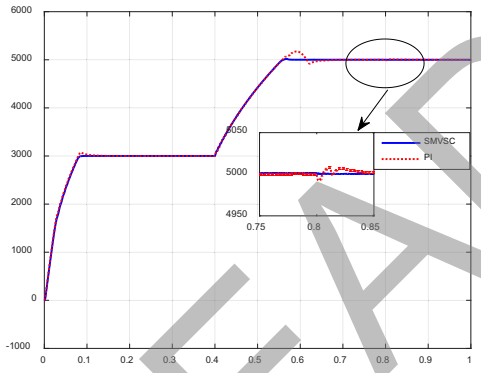

Fig. 4: Speed response curves comparison of interference in the high speed condition

From Fig.4, it can be known that the proposed control strategy shows good performance under the sudden load interference simulation in the above base speed condition. Overshoot is about 0.2% and transition time is about 0.028s when PI control strategy is applied while no change is in the speed response curve when SMVSC and flux-weakening control strategy is applied. Hence, anti-disturbance performance and robustness of the PMSM system are strengthened through applying the SMVSC and flux-weakening control strategy.

7 Conclusion

In this paper, the control strategy based on SMVSC algorithm and flux-weakening control algorithm is applied to the vector control system of PMSM for the electric vehicles. The delay problem caused by the introduction of integral link in the SMVSC algorithm is solved by using the method of the integrated signal times the saturation function. Through this research, the good anti-jamming capability is achieved and the working conditions requirement of wide speed range is met.

References

[1] Sun Qiang, Cheng Ming, Zhou E, Hu Minqiang. Variable PI control of a novel doubly salient permanent magnet motor drive[J]. Proceedings of the CSEE, 2003, 23(6): 117-123.

[2] Chiu-Keng Lai, Kuo-Kai Shyu. A novel motor drive design for incremental motion system via sliding-mode control method[J]. IEEE Trans. On Industrial Electronics, 2005, 52(2): 499-507.

[3] Bossanyi E A. GH bladed theory manual[R]. UK-Bristal: Grand Hassan and Partner Limited, 2009: 13-36.

[4] Gong Xianwu, Xu Shufen, ZHANG Lijun, Wang Guiping. Research on Permanent Magnet Synchronous Motor Fuzzy Adaptive Compensation Control System[J]. Computer Simulation, 2014,31(1): 356-360.

[5] Wang haibo, Zhou Bo, Fang Sichen. A PMSM sliding mode control system based on exponential reaching law[J]. Transactions of China Electrotechnical Society, 2009,27(9): 71-77.

[6] Zhang Xiaoguang, Sun Li, Zhao Ke. Sliding mode control of PMSM based on a novel load torque sliding mode observer[J]. Proceedings of the CSEE, 2012,32(3):111-116.

[7] Liu Ying, Zhou Bo, Fang Sichen. Sliding mode control of PMSM based on a novel disturbance observer [J]. Proceedings of the CSEE, 2010,30(9):80-85.

[8] Liu Qinghua, LV Yongjian, Yangjie. Sliding Mode Variable Structure Control of Electric Vehicles PMSM[J]. Computer Simulation, 2015,32(12): 129-132.

[9] Seok- Hee Han, Wen L. Soong. Reducing Harmonic Eddy-Current Losses in the Stator Teeth of Interior Permanent Magnet Synchronous Machines During Flux Weakening[J]. Transactions on Energy Conversion, 2010,2:473-478.

[10] Ma Guifang, Zhang Kafei, Chen Yang. A leading angle flux-weakening control of permanent magnet synchronous motor used in electric vehicles[J]. Journal of Nanchang University(Engineering & Technology), 2016,38(2): 196-199.

[11] Tang Zhaohui, Ding Qiang, Yu Shouyi, Gui Weihua. Research of Flux Weakening Strategy of an Surface Mounted Permanent Magnet Synchronous Motor[J]. Control Engineering of China, 2011,18(3): 384-387.

[12] Roberto Petrella. Feed forward Flux-Weakening Control of Surface Mounted Permanent Magnet Synchronous Motors Accounting for Resistive Voltage Drop [J]. IEEE Transactions on Industrial Electronics, 2010, 57(1): 440-448.

[13] Wang Yan, Zhang Ze, Qin Xuqing. Modeling and control for hydraulic transmission of unmanned ground vehicle[J]. Journal of Central South University, 2014, 21(1): 124-129.

[14] Zhang Xiaoguang, Zhao Ke, Sun Li, An Quntao. Sliding mode control of permanent magnet synchronous motor based on a novel exponential reaching law[J]. Proceedings of the CSEE, 2011, 31(15): 47-52.

[15] Tae-suk Kwon, and Seung-Ki Sul. A novel flux weakening algorithm for surface mounted permanent magnet synchronous machines with infinite constant power speed ratio[C]. Proceeding of International Conference on Electrical Machines and Systems, ICEMS 2007: 440-445.